Neurobiology of Aging 134 (2024) 84–93

Contents lists available at ScienceDirect

Neurobiology of Aging

journal homepage: www.elsevier.com/locate/neuaging.org

Regular article

Identifying potential genetic epistasis implicated in Alzheimer's disease via detection of SNP-SNP interaction on quantitative trait CSF $A\beta_{42}$

Jin Li [a,†], Dandan Chen [a,b,†], Hongwei Liu [a], Yang Xi [c], Haoran Luo [a], Yiming Wei [a], Junfeng Liu [c], Hong Liang [a,*], Qiushi Zhang [c,**]

[a] College of Intelligent Systems Science and Engineering, Harbin Engineering University, Harbin, China
[b] School of Automation Engineering, Northeast Electric Power University, Jilin, China
[c] School of Computer Science, Northeast Electric Power University, Jilin, China

ARTICLE INFO

Keywords:
Amyloid-β_{42} ($A\beta_{42}$)
ADNI
Alzheimer's disease
Epistasis
PPI

ABSTRACT

Although genome-wide association studies have identified multiple Alzheimer's disease (AD)-associated loci by selecting the main effects of individual single-nucleotide polymorphisms (SNPs), the interpretation of genetic variance in AD is limited. Based on the linear regression method, we performed genome-wide SNP-SNP interaction on cerebrospinal fluid $A\beta_{42}$ to identify potential genetic epistasis implicated in AD, with age, gender, and diagnosis as covariates. A GPU-based method was used to address the computational challenges posed by the analysis of epistasis. We found 368 SNP pairs to be statistically significant, and highly significant SNP-SNP interactions were identified between the marginal main effects of SNP pairs, which explained a relatively high variance at the $A\beta_{42}$ level. Our results replicated 100 previously reported AD-related genes and 5 gene-gene interaction pairs of the protein-protein interaction network. Our bioinformatics analyses provided preliminary evidence that the 5-overlapping gene-gene interaction pairs play critical roles in inducing synaptic loss and dysfunction, thereby leading to memory decline and cognitive impairment in AD-affected brains.

1. Introduction

Alzheimer's disease (AD) is a devastating neurodegenerative disorder with high prevalence, which contributes to a substantial public health problem (Abdullah et al., 2022; The Texas Alzheimer Research and Care Consortium et al., 2012). Worldwide estimates of prevalence vary, with an estimate of 35–50 million individuals worldwide afflicted with AD or other dementia, which is expected to rise to 132 million by 2050 (Hassan and Kerman, 2019; Meyers et al., 2022; Ridge et al., 2013). Therefore, the urgency of the global challenge of AD has led to increased efforts over the past decade to better understand the AD progression. Although tremendous progress has been made in understanding the pathogenesis of AD which is influenced by genetic factors, the genetic mechanisms of AD are still unclear (Sims et al., 2020; The Texas Alzheimer Research and Care Consortium et al., 2012; Wang et al., 2021). Early diagnosis of AD prior to the development of significant clinical symptoms remains a top priority of research (Bondi et al., 2008).

Over the past decades, traditional genome-wide association studies (GWAS) have identified dozens of AD-associated loci by selecting the main effects of individual single-nucleotide polymorphisms (SNPs), yet all these are accountable for only a fraction of the estimated heritability, suggesting that a large portion of the genetic components of AD remain unexplained (Hu et al., 2020; Lu et al., 2018; Miron et al., 2018; The Texas Alzheimer Research and Care Consortium et al., 2012; Vance et al., 2020). Therefore, researchers have conducted studies on the genetics of AD using multiple methods and databases in recent years, and their findings are a step forward in identifying the genetic factors that contribute to AD risk. For example, although additive main effects of significant SNPs are considered in subsequent large-scale GWAS with the recent explosion in high-throughput genotyping technology, these results were still challenged for "missing heritability" (Jansen et al., 2019).

Epistasis is the interaction of genetic variation at 2 or more loci during the expression of a single phenotype, in which the effects of a

* Correspondence to: College of Intelligent Systems Science and Engineering, Harbin Engineering University, 145 Nantong Street, Harbin, China.
** Correspondence to: School of Computer Science, Northeast Electric Power University, 169 Changchun Street, Jilin 132012, China.
E-mail addresses: lh@hrbeu.edu.cn (H. Liang), 48526754@qq.com (Q. Zhang).
† These authors contribute equally.

https://doi.org/10.1016/j.neurobiolaging.2023.10.003
Received 22 June 2023; Received in revised form 6 October 2023; Accepted 10 October 2023
Available online 17 October 2023

given gene on a biological trait are masked or enhanced by one or other genes (Mackay, 2014; Moore, 2005). This type of interaction plays a critical role in explaining the missing heritability of complex diseases, and many of the unexplained genetic factors affecting AD etiology may be epistatic (Abd El Hamid et al., 2022; Cavalcante et al., 2022; Chen et al., 2021). Therefore, going beyond single-marker analysis is necessary to look for epistatic relationships that might contribute to explaining the "missing heritability" of AD (Hohman et al., 2013). Notably, current studies on genome-wide SNP-SNP interactions in AD pathology are scanty and typically focus on SNPs that have significant individual effects. However, considering the uncertainty of that kind of interaction, we cannot disregard the possibility of significant SNP-SNP interaction between SNPs with marginal main effect (Hibar et al., 2015). Therefore, to solve the issue of missing some significant SNP-SNP interactions due to ignoring insignificant single SNPs, detecting SNP-SNP interaction across the whole genome is necessary. Overall, detecting genome-wide SNP-SNP interaction will be conducive to novel signal mining, which could partially explain the "missing heritability" of AD (Li et al., 2015).

Owing to the ultra-high dimension of SNP datasets, detecting SNP-SNP interactions across the whole genome is a computationally expensive challenge. To address this issue, a total of 105 methods to detect epistasis have been published between 2010 and 2020 by Web of Science (Abd El Hamid et al., 2023; Russ et al., 2022; Wang et al., 2023). The methods have been classified into 3 types: exhaustive search methods, data mining approaches, and swarm intelligence methods, and most of them have been designed for case-control tasks, with few on quantitative trait (QT). Moreover, these methods mostly choose to refrain from the brute force search in the SNP-SNP interaction space and try to reduce computational burden using dimensionality reduction screening and priori knowledge. However, using more subjective priori knowledge or random factors for dimension reduction search will lead to signal loss because the risk of epistatic interaction is unknown.

Compared to discrete case-control status, continuous QT has higher statistical power to better track pathophysiological processes in AD and could contribute to detecting potential risk variants related to QT at the same time (Li et al., 2017). Pathologically, AD is characterized by the existence of extracellular senile plaques, intracellular neurofibrillary tangles (NFTs), and the loss of synapses and neurons, resulting in global cognitive decline and eventually dementia (Congdon and Sigurdsson, 2018). As a 39–43 residue amphipathic peptide, the amyloid β-peptide (Aβ) is the major proteinaceous component of the extracellular senile plaque (Quon et al., 1991). The major Aβ species found in vivo are $A\beta_{1-40}$ and $A\beta_{1-42}$, which are composed of 40 and 42 residues, respectively. By contrast, $A\beta_{1-42}$ has 2 additional hydrophobic residues, Ile41 and Ala42, yet it shows remarkably faster aggregation and greater neurotoxicity than $A\beta_{1-40}$ (Nguyen et al., 2016; Zhang et al., 2002). Imprecise cleavage of the amyloid precursor protein substrate by γ-secretase affects the relative amounts of 2 main Aβ fragments: amyloid-β_{42} ($A\beta_{42}$) and amyloid-β_{40} ($A\beta_{40}$). In the Alzheimer's disease neuroimaging initiative (ADNI) clinical dataset, there are only 3 cerebrospinal fluid (CSF) biomarkers available: tau, $A\beta_{42}$, and P-tau181P, while $A\beta_{40}$ is not included in the dataset. As one of the 3 core and predictive CSF biomarkers, $A\beta_{42}$ has been included in the diagnostic criteria of AD and is playing an increasing and important role in predicting the progression from a prodromal stage of AD to AD (Law et al., 2018; Li et al., 2018; Marchegiani et al., 2019). In recent years, the utilization of $A\beta_{42}$ on AD has produced many achievements. For example, distinct regional patterns of Aβ burden are valuable biomarkers for assessing the risk of disease progression in cognitively normal and mild cognitive impairment (Pfeil et al., 2021). Intervention before Aβ reaches pathological levels is an obvious benefit (Elman et al., 2020). rs9357347 reduces the risk of AD by modulating Aβ pathology and neuronal degeneration (Tian et al., 2019). $A\beta_{42}$ is highly correlated with other biomarkers and might help in reducing the risk of early mild cognitive impairment or late mild cognitive impairment in amyloid-negative patients (He et al., 2021). Furthermore, studies using brain-derived soluble Aβ oligomers in AD have suggested that principally small and diffusible oligomers can disrupt synaptic plasticity (Li and Selkoe, 2020). Soluble Aβ oligomers disrupt synaptic function and prevent the formation of soluble Aβ oligomers much more than do fibrillar amyloid plaque cores or Aβ monomers, which could be a novel therapeutic avenue for AD (Li et al., 2018). As aforementioned, mining more potential loci by $A\beta_{42}$, which are implicated in AD without ignoring the factor of underlying genetic interaction across the whole genome, is urgently needed.

In our study, we performed a genome-wide epistasis detection study in the ADNI cohort and bioinformatics analyses for the results interpreting to discover potential genetic epistasis implicated in AD. CSF $A\beta_{42}$ was used as a QT to advance statistical power and biological interpretation.

2. Materials and methods

2.1. Participants

This study involved 1178 individuals from the ADNI database, which included 3 stages: ADNI 1, ADNI GO, and ADNI 2. A total of 6,187,414 SNPs from all these 1178 individuals participated in the subsequent quality control (QC). For this study, stringent QC was performed on participants using PLINK v.1.9 software. SNPs were selected from the genotypic data based on certain and clear criteria. We first selected SNPs that were distributed on chromosomes 1–22. The next requirement for SNPs and participants concerned the minimum call rate: the minimum call rate ≥95% were selected. The minor allele frequency should no smaller than 5%. The Hardy-Weinberg equilibrium test *p*-value should no smaller than 10^{-6}. Then, a total of 563,980 SNPs from 1079 participants passed QC. The CSF $A\beta_{42}$ phenotype was used in this study. The presence of Aβ plaques and NFTs has been regarded as the main pathological hallmark of AD (Armstrong, 2009). Related studies have shown that $A\beta_{42}$, P-tau, and T-tau are key biomarkers of CSF for pathophysiology in AD. $A\beta_{42}$ has been widely studied and has important implications for studying the association between genotype and AD. QC of the CSF $A\beta_{42}$ process was based on 2 principles: baseline consistency and normal distribution. Among the remaining 1079 participants, only 843 participants had both genotype data and phenotype (CSF $A\beta_{42}$) after QC. These participants (N = 843) included 199 cognitive normal cognitions, 85 significant memory impairments, 239 early mild cognitive impairments, 207 late mild cognitive impairments, and 113 AD participants. After QC, 843 valid $A\beta_{42}$ of CSF participants and 563,980 SNPs qualified for subsequent genome-wide SNP-SNP interaction analyses.

2.2. Model of SNP-SNP interaction detection

SNPs are high-density bi-allelic markers with allele A and a, where a lowercase letter denotes the minor allele, and an uppercase letter denotes the major allele. Each SNP thus has only 3 genotypes: 2 homozygous genotypes (AA and aa) and 1 heterozygous genotype (Aa). Therefore, we detected the SNP-SNP interaction by including each SNP coded as (0,1,2) for (homozygote common allele, heterozygote, homozygote rare allele), respectively.

In this study, we performed a genome-wide SNP-SNP interaction detection using a linear regression framework. We included age, gender, and diagnosis (dx) as covariate terms in the linear regression models for $A\beta_{42}$, to control for any factors outside of genetics that may influence AD. The model of additive main effect of SNP_1 and SNP_2 is defined as:

Additive model:

$$f = \alpha + \beta_1 \times SNP_1 + \beta_2 \times SNP_2 + \beta_3 \times age + \beta_4 \times gender + \beta_5 \times dx \quad (1)$$

SNP × SNP model：

$$f = \alpha + \beta_1 \times SNP_1 + \beta_2 \times SNP_2 + \beta_3 \times age + \beta_4 \times gender + \beta_5 \times dx + \beta_6 \times I_{SNP_1 \times SNP_2} \quad (2)$$

where α, β_1, β_2, β_3, β_4, β_5, and β_6 are regression coefficients. The SNP × SNP model consisted of the same SNP and covariate terms as the additive model, while with an additional multiplicative interaction term for the SNP × SNP model. To attack the intensive computational burden caused by the exponential growth of the search space in SNP-SNP interaction detection, a multi-GPU-based method was used for parallel computing (Zhang et al., 2022). After solving the models, the *p*-value of the interaction effects is given by the F-test statistic, which can be calculated as:

$$p - value = P(F > F_{sta}) = 1 - F_n(F_{sta}, df_1, df_2) \quad (3)$$

where F_n is the probability density function of the beta distribution, F_{sta} is the F-test statistic, df_1 is the freedom degree of the interaction term, and df_2 is the freedom degree of the independent variable in the model.

2.3. Statistical analyses

A linear regression model was used to evaluate the effects of genome-wide SNP-SNP interactions. First, the main genetic effect was added, followed by the addition of genetic interaction term to determine the variance associated with the interaction term alone. Epistatic interactions with Aβ$_{42}$ as QT were detected, while 3 factors, including age, gender, and diagnosis, were included as covariates in the linear regression analysis. The epistasis interaction detection adds interaction term to the additive effects of 2 SNPs and calculates the *p*-value of the interaction factors. Approximately 159 million unique SNP pairs were detected in this epistasis interaction work, and 318 billion regressions were calculated.

Functional enrichment was analyzed using the Enrichr online tool to reveal biological implications at the gene level. Enrichr is a comprehensive gene set enrichment analysis web server for biological discoveries that enables querying hundreds of thousands of annotated gene sets. The Enrichr platform is a comprehensive online tool for gene enrichment analysis that contains many genome annotation libraries that can be used for analysis and download, such as transcription, pathways, ontologies, diseases/drugs, cell types. The output results of Enrichr database include the result tables and results of multiple visualizations, such as bar charts, grid maps, network graphs, and cluster heatmaps, which can be used for presentation (Kuleshov et al., 2016; Xie et al., 2021). In this study, PhenGenI (Al-Shammari et al., 2022) and DisGeNET (Piñero et al., 2019) databases from the diseases/drugs libraries of the Enrichr tool were used for functional and pathway enrichment analyses. In PhenGenI enrichment analysis and DisGeNET enrichment analysis, the top 10 significant pathway enrichment was taken as the selection criterion. For statistical importance of the enrichment results, the upper threshold for the adjusted *p*-value was set at 0.05 (Islam et al., 2022).

To further investigate the biological functions and its biological implications of the results, a protein-protein interaction (PPI) network was constructed using the STRING tool (https://string-db.org/, accessed on October 20, 2022). Nodes and edges in the PPI network represent the genes (proteins) and the interactions between 2 genes, respectively. By determining the correlation between genes through the edges between nodes, we understand the relationship between genes and analysis potential genetic epistasis implicated in AD. STRING is a database on PPI, covering most species and containing the highest information on interaction. The analysis of PPI plays a critical role in predicting genotype-phenotype associations in complex diseases. PPI networks are useful resources for identifying protein interactions and efficiently mapping all the interactions of a given organism's proteome gathered from the literature through systematic mining (Safari-Alighiarloo et al., 2014). Moreover, the visualization of gene-gene interaction pairs was generated in the form of chord diagram using the online tool Bioladder (https://www.bioladder.cn/, accessed on December 18, 2022). In addition to manual search, we also used PubMed and Google Scholar to search for articles showing any interesting relationships between our identified gene-gene interaction pairs that overlap with the PPI network to AD.

3. Results

3.1. SNP-SNP interaction results

In this study, we analyzed genome-wide SNP-SNP interaction on the Aβ$_{42}$ intermediate phenotype using a GPU-based linear regression model with age, gender, and diagnosis as covariates. A total of 368 pairs of SNPs were identified and showed statistically significant interaction with Aβ$_{42}$ level. The interactive and main effects of the 368 significant SNP-SNP interaction pairs are shown in Fig. 1. All pairs of 368 SNP-SNP interactions shared common characteristics in that the interaction effects were much higher than the main effect. Significant SNP-SNP interaction was detected among the SNPs with marginal main effect.

To further confirm the association of SNP-SNP interaction detected in this study, IBM SPSS 24.0 was used to calculate the variance explained by each identified SNP after controlling age, gender, and diagnosis as covariates. The variances were calculated for the additive and interaction terms separately using 2 hierarchical linear regression models. The significance validation of SNP-SNP interaction was analyzed using the SPSS general linear model, and R-squared of the interaction and additive terms are shown in Fig. 2.

The top 10 R-squared values of SNP-SNP interaction pairs are shown in Table 1. The interaction term was finally incorporated, which was used to compute additional variance. As shown in Table 1, for each identified SNP-SNP interaction pair, the variance proportion of the interaction term is much higher than that of the main effects. The highest percent was 6% after combined the interaction term of $SNP_1 \times SNP_2$ and main effect of $SNP_1 + SNP_2$. For example, the interaction term accounted for 5.6% of the variance, and the main effects accounted for 0.4% of the variance (6.0% combined) in rs6463343 (**SLC29A4*)-rs4757417 (*SOX6*). As we expected, these interaction pairs all had marginal main effects but explained a relatively high-level variance of Aβ$_{42}$. In addition, the previously reported AD risk genes were replicated in our study: *NFIA*, *MYH9*, *CARD11*, *KCNA6*, *TRAM2*, *SCARB1*, *NIPSNAP3B*, *CDH9*, and *C8orf34*, as shown in bold italics in Table 1. These results were obtained after searching through the Enrichr online tool.

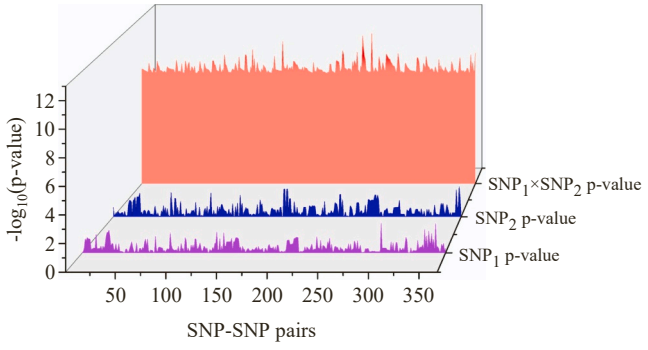

Fig. 1. The 3D waterfall plot for interaction effects and main effects of each SNP with $-\log_{10}$ (*p*-values). The number of significant SNP-SNP pairs was 368. For each interaction pair, the orange waterfall represents main effects of SNP_1; the purple waterfall represents main effects of SNP_2; and the red waterfall represents the interaction effects of SNP_1-SNP_2 pairs. Abbreviations: SNP, single-nucleotide polymorphism.

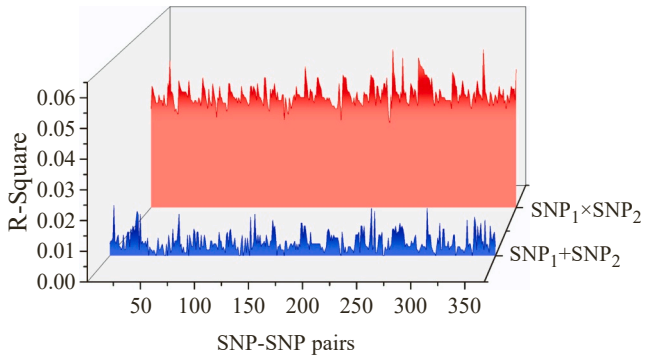

Fig. 2. The 3D waterfall plot for interaction and additive terms with R square in the linear regression model. The red area represents the variance explained by the interaction term on $A\beta_{42}$. The blue area represents the variance explained by the additive term on $A\beta_{42}$. Abbreviations: SNP, single-nucleotide polymorphisms.

3.2. Functional enrichment analysis results

The identified SNPs were mapped onto the genome by *Homo sapiens* genome assembly *GRCh37* (hg19) to analyze further the biological significance at the gene level. In total, 368 SNP-SNP pairs that included 567 SNPs were mapped onto 103 gene-gene pairs (including 199 different genes). In addition, we found that 100 genes out of 199 genes were included in the items related to AD by searching in 2 gene set libraries of Enrichr: PhenGenI_Association_2021 and HDSigDB_Human_2021, which indicated that they were reported as AD-related genes. However, the other 99 genes have not been found in the items related to AD based on the gene set libraries of PhenGenI_Association_2021 and HDSigDB_Human_2021, which suggested that they were not yet reported as AD-related genes. In this study, the relationship between gene-gene pairs and AD was divided into 3 sets: set-I, set-II, and set-III, as shown in Fig. 3. In set-I, 2 genes in each pair are AD-related genes, and in set-II, only 1 gene in each pair is an AD-related gene. The peculiar feature of set-III is that neither of the 2 genes in each pair is associated with AD.

To further illustrate the correlation between the identified genes and AD, we performed gene set enrichment analyses using PhenGenI and DisGeNET databases. Using PhenGenI disease enrichment analysis, we found that the item of "Alzheimer disease" ranked in top 10. The top 8 enriched PhenGenI pathways were cholesterol and high-density lipoprotein, platelet function tests, echocardiography, electrocardiography, stroke, triglycerides, resistin, and Alzheimer disease, as shown in Fig. 4A. Intriguingly, the cholesterol and high-density lipoprotein pathway was reported to be directly related to AD (Puglielli et al., 2003; Shobab et al., 2005). Moreover, the top 4 enriched DisGeNET pathways were unipolar depression, schizophrenia (SZ), major depressive disorder, and Alzheimer disease and late onset, as shown in Fig. 4B. Using DisGeNET disease enrichment analysis, we found that the significant enrichment pathways include major psychiatric disorders such as unipolar depression, SZ, and major depressive disorder, as well as neurodegenerative disorder, such as Alzheimer disease. Noteworthy, depression and SZ are related to the occurrence and development of AD indirectly (Ashe et al., 2001; Ownby et al., 2006). Researchers have suggested that psychotic symptoms affect a sizable proportion of individuals with AD and persistent in AD patients (Ropacki and Jeste, 2005).

3.3. Protein-protein interaction network analysis

To further interpret biological implications at the level of gene-gene interactions, all the 103 pairs of gene-gene interaction, which from set-I (Fig. 3A), set-II (Fig. 3B), and set-III (Fig. 3C) were used to analyze the PPI network. Based on the STRING tool, a PPI subnetwork with 10 genes and 17 interaction pairs was identified. The chord diagram was generated using the online server BioLadder (https://www.bioladder.cn/, accessed on December 18, 2022) to visualization the analysis of gene-gene interaction pairs. The different colored regions and colored curves in the chord diagram represent the genes and the interactions between 2 genes, respectively, as depicted in Fig. 5. The 10 genes were *APP*, *MYH9*, *ITGB3*, *AUTS2*, *SORBS1*, *ITPR2*, *FMN2*, *SPHKAP*, *SH3BP4*, and *DLG2*. As a result, 5 pairs overlapped with the PPI network in this study, as shown by the purple curves in Fig. 5, which were *APP-ITPR2*, *MYH9-ITGB3*, *DLG2-SH3BP4*, *FMN2-SPHKA*, and *SORBS1-AUTS2*, and their biological implications deserve further discussion.

Table 1
Top10 R square of SNP-SNP interaction pairs

No.	$SNP_1 \times SNP_2$	Gene	CHR	*p*-value		Explained variance (R square)		
				GWAS	Interaction	Age + gender + dx[a]	$SNP_1 + SNP_2$[b]	$SNP_1 \times SNP_2$[c]
1	rs6463343	[d]*SLC29A4*	7	0.352	1.15E−09	0.149	0.004	0.056
	rs4757417	*SOX6*	11	0.428				
2	rs6686758	***NFIA***	1	0.723	1.48E−09	0.149	0.003	0.052
	rs2718293	[d]*SLC66A2P1*	7	0.766				
3	rs1005570	***MYH9***	4	0.438	6.39E−11	0.149	0.003	0.049
	rs12603582	*ITGB3*	18	0.542				
4	rs12531570	[d]***CARD11***	7	0.302	2.96E−12	0.149	0.003	0.048
	rs11600150	[d]*MRGPRX1*	11	0.947				
5	rs1003564	[d]**KCNA6**	12	0.451	1.43E−10	0.149	0.007	0.048
	rs12246684	*CCDC172*	10	0.624				
6	rs1003564	[d]***KCNA6***	12	0.451	1.64E−10	0.149	0.007	0.047
	rs12244656	*CCDC172*	10	0.615				
7	rs2268731	***TRAM2***	6	0.876	8.52E−11	0.149	0.001	0.046
	rs701106	***SCARB1***	12	0.821				
8	rs4683427	*PLS1*	3	0.098	9.07E−11	0.149	0.008	0.046
	rs12552611	[d]***NIPSNAP3B***	9	0.121				
9	rs6870789	***CDH9***	5	0.505	2.84E−10	0.149	0.005	0.046
	rs1434927	***C8orf34***	8	0.235				
10	rs1382932	***CDH9***	5	0.487	3.09E−10	0.149	0.005	0.046
	rs1434927	***C8orf34***	8	0.235				

Key: GWAS, genome-wide association studies; SNP, single-nucleotide polymorphisms.
[a] Age + gender + dx: percent variance in $A\beta_{42}$ levels explained by age, gender, and dx.
[b] $SNP_1 + SNP_2$: percent additional variance in $A\beta_{42}$ levels explained by the combined main effect of SNP_1 and SNP_2 after accounting for age, gender, and dx.
[c] $SNP_1 \times SNP_2$: percent additional variance in $A\beta_{42}$ levels explained by the interaction effect of SNP_1 and SNP_2 after accounting for age, gender, dx, SNP_1, and SNP_2.
[d] Nearest gene proximal to SNP.

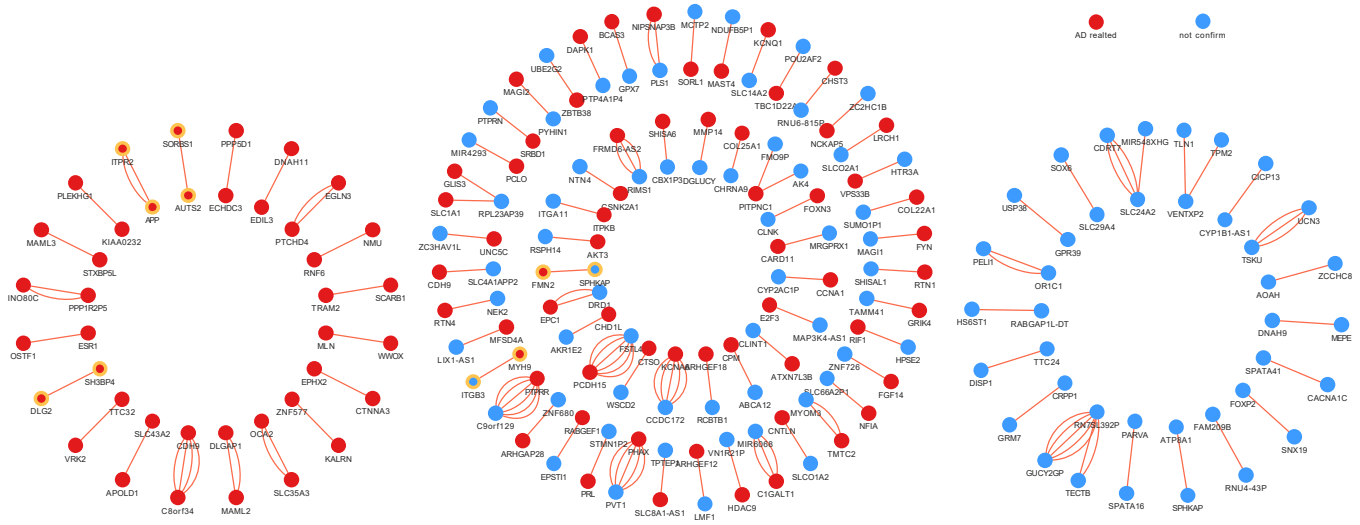

Fig. 3. Three sets of relationship between a gene-gene interaction pair and AD based on the Enrichr: (A) Set-I of the first relationship includes 20 pairs of gene-gene interaction and 40 different genes; both genes in each pair are AD related; (B) set-II of the second relationship includes 62 pairs of gene-gene interaction and 122 different genes; only 1 gene in each pair is AD-related; (C) set-III of the third relationship includes 21 pairs of gene-gene interaction and 39 different genes; none in each pair is associated with AD. The red spots represent previously reported AD-related genes. Genes represented by blue spots have not been reported association with AD. Among them, there are 2 or even more than 2 lines between the 2 spots, which represents more than 1 pair of SNP mapping on the same pair of genes. The gene pairs highlighted in yellow represent the identified 5 pairs of gene-gene interaction that overlapped with the PPI network in this study. Abbreviations: AD, Alzheimer's disease.

In addition, the 5 gene pairs were mapped by 6 SNP-SNP interaction pairs: rs11576138-rs6760875, rs1005570-rs12603582, rs12698823-rs12247017, rs440666-rs1386810, rs440666-rs4964017, and rs6738858-rs12291567. The mean $A\beta_{42}$ is plotted against each pairwise genotype combination of 6 SNP pairs with significant genome-wide interaction, as shown in Fig. 6. The colored bars in Fig. 6 represent pairwise genotype combinations of SNP_1-SNP_2 interactions. The results showed that different genotype combinations may be contribute to the phenotypic changes, thereby increasing the risk of incident AD.

4. Discussion

From 60% to 80% of AD risk is reported to be associated with genetics. Although GWAS for AD have identified multiple SNPs in genes associated with AD risk, the problem of "missing heritability" in AD remains serious (Zajac et al., 2023). Epistasis has been considered a prime cause of "missing heritability" in AD in recent years. To study such complex diseases, it is necessary to detect epistasis to unraveling the underlying relationship between genotypes and AD-related phenotypes. Therefore, this study focused on identifying epistasis between 2-marker interactions at marginal main effects across the whole genome. To our knowledge, this genome-wide study is a highly comprehensive epistatic detection of QT at the $A\beta_{42}$ level. A total of 368 SNP pairs were found to be statistically significant.

At the level of SNP-SNP interaction, all 368 SNP-SNP pairs showed statistical significance, and highly significant SNP-SNP interactions were detected between SNPs with marginal main effect. In particular, the interaction effects were much higher than the main effects (Fig. 1). As we expected, all identified interaction pairs explained a relatively high-level variance at the $A\beta_{42}$ level (Fig. 2 and Table 1), which could be helpful for explaining some part of the "missing heritability" of AD.

After gene source annotation using the online tool Enrichr, 103 gene pairs (including 199 different genes) were divided into 3 sets according to the relationship of gene-gene pair with AD. Among 199 different genes, 100 were AD-related, and 99 were not confirmed as AD-related. The results are more abundant than those of our previous GWAS (Li et al., 2017) and have higher correlation and replication rates. Most of the identified genes were enriched in AD or AD-related diseases. Therefore, our results can efficiently identify AD-related genes and potential genes implicated in AD.

At the level of gene-gene interaction, 82 gene-gene interaction pairs, including those from set-I (Fig. 3A) and set-II (Fig. 3B), were used to perform PPI network analysis using the STRING database. Analysis of PPI networks is being increasingly recognized as an effective way to obtain biologically meaningful explanations, which helps in characterizing the underlying biology of genes associated with complex diseases (Safari-Alighiarloo et al., 2014). Therefore, this study performed PPI network analysis utilizing the online search tool STRING. As shown in Fig. 5, the PPI subnetwork containing 10 genes and 17 gene-gene interactions was identified. As a result, 5 gene-gene interaction pairs overlapped with the PPI network and need further discussion.

Amyloid precursor protein (*APP*) originates from Aβ that is a major component of extracellular plaques found in AD brains. Aβ aggregation leading to amyloid plaque deposition is the main pathological feature of AD, and *APP* increases the possibility of Aβ aggregation and early onset AD (Bharadwaj et al., 2009; Dorostkar et al., 2015). *APP* promotes synaptic activity, and the formation of synapses and dendritic spines, and plays a pivotal role in memory and learning (Rajmohan and Reddy, 2017). The accumulation of C-terminal fragments of *APP* causes synaptic failure and memory impairment, which is a possible cause of AD (Kametani and Hasegawa, 2018). Inositol 1,4,5-trisphosphate receptor type 2 (*ITPR2*) is a protein-coding gene, which has been shown to be associated with AD risk. Astrocytes regulate synapse elimination through an *ITPR2*-dependent manner (Yang et al., 2016), and increased expression of *ITPR2* could lead to neuronal calcium toxicity and cell death (Mencer et al., 2021). Therefore, *APP-ITPR2* interaction might induce synaptic damage in AD neurons and may be related to synapse elimination. Furthermore, synaptic damage and loss are fundamental to the pathophysiology of AD and are also a key change in the synapse during AD progression, which leads to reduced cognitive function (John and Reddy, 2021; the Synaptic Health Endpoints Working Group et al., 2020).

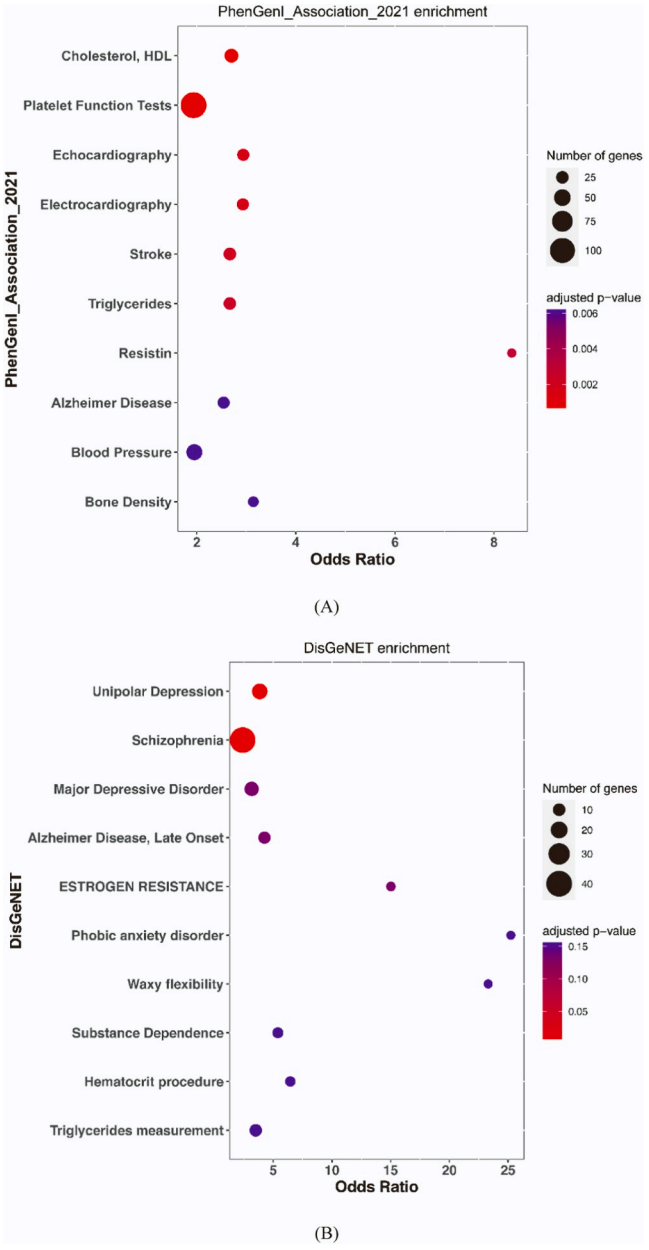

Fig. 4. Bubble plot presentation of enriched PhenGenI Association 2021 enrichment and DisGeNET enrichment ranked according to adjusted *p*-values. (A) Enriched PhenGenI terms ranked top 10 according to adjusted *p*-values. (B) Enriched DisGeNET terms ranked top 10 according to adjusted *p*-values. Numbers of genes contributing to each term are displayed as dots.

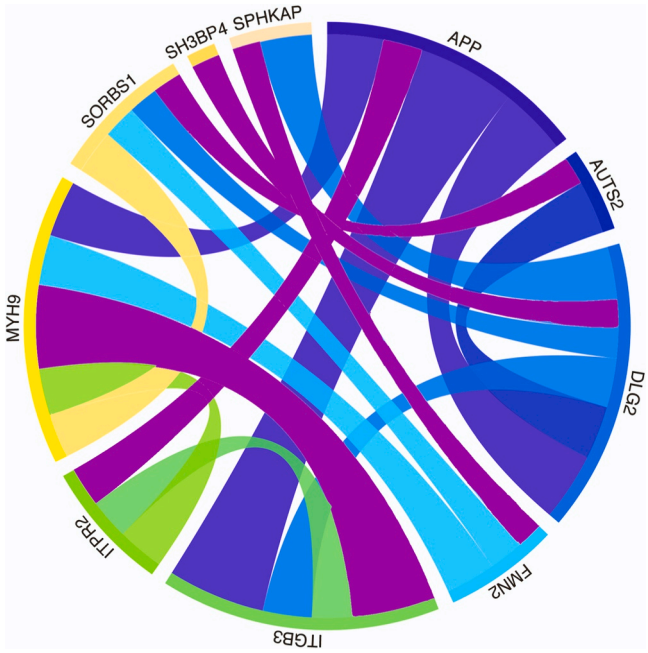

Fig. 5. Chord diagram of the protein-protein interaction (PPI) subnetwork (with 10 genes and 17 interactions) generated by BioLadder and STRING. The purple curves represent the 5-overlapping gene-gene pairs in the PPI network. The thickness of the curves represents the combined score of evidence that suggesting a functional link in PPI network: the thicker the curves is, the more important this connection is. Abbreviations: APP, amyloid precursor protein; AUTS2, autism susceptibility candidate 2; DLG2, disks large homolog 2; FMN2, formin-2; ITGB3, integrin alpha-V/beta-3; ITPR2, inositol 1,4,5-trisphosphate receptor type; MYH9, myosin heavy chain 9.

Myosin Heavy Chain 9 (*MYH9*) is a previously reported gene correlated with AD risk. Acting as a regulator of actin cytoskeleton, *MYH9* interacts with actin and participates in various biological processes. *MYH9* expression is decreased in NFTs accumulated by tau, while tau functions have been suggested to be downstream of Aβ in the hypothesis of amyloid plaques and tau tangles (Hondius et al., 2021; John and Reddy, 2021; Smith et al., 2019). Integrin alpha-V/beta-3 (*ITGB3)* gene is a susceptibility region for AD. Integrins play an important role in maintaining and modulating neuronal synaptic activity (Sethi and Zaia, 2017). Moreover, the number of dendritic spines is related to actin, and dendritic spines are the major site of synapse formation among neurons (Bosch and Hayashi, 2012). Based on the above analysis, *MYH9-ITGB3* interaction might be related to the modulation of synaptic activity and may be helpful for the development of the nervous system.

Disks large homolog 2 (*DLG2*) is a novel AD-associated gene involved in regulating synaptic stability and part of the postsynaptic protein scaffold of excitatory synapses. Downregulation of synaptic scaffolding proteins has been described as an early event in AD. Reduced expression of *DLG2* has been noticed in AD patients (Prokopenko et al., 2022). Moreover, *DLG2*, also known as postsynaptic density protein 93 (*PSD93*), attenuates amyloid-β-mediated cognitive dysfunction by promoting the catabolism of Aβ (Yu et al., 2017). SH3 domain-binding protein 4 (*SH3BP4*) is involved in lectin-mediated endocytosis controlled by cargo. Lectin-mediated endocytosis is an indispensable step in cellular regulation, and endocytosis plays a direct role in the processing of *APP*. Reduced synaptic accumulation of Aβ may reduce synaptic loss and enhance cognitive function in AD patients (Smith et al., 2019). Therefore, *DLG2-SH3BP4* interaction may correlate with synaptic and cognitive functions during AD progression.

Formin-2 (*FMN2*) has been implicated in regulating actin dynamics. *FMN2* is deregulated in patients with AD, and chronically reduced levels of *FMN2* accelerate age-related memory decline. Lack of *FMN2* could result in a corresponding impairment in synaptic plasticity in young mice (Agís-Balboa et al., 2017). The sphingosine kinase 1 interactor, AKAP domain containing (*SPHKAP*) is a protein-coding gene. Neurons in the brains of patients with AD show a decrease in sphingosine kinase 1, which could lead to defects in microglial phagocytosis and dysfunctional resolution of inflammation. Neuroinflammation has also been proposed to provide a link between early Aβ pathology and subsequent NFT formation. Moreover, AD-related inflammatory signals can modify the ramified morphology of microglia, thereby resulting in synaptic loss and dysfunction (Piccioni et al., 2021). Overall, *FMN2-SPHKAP* interaction might play a critical role in inducing synaptic loss and dysfunction or may be related to neuroinflammation, thereby leading to memory decline and cognitive impairment.

SORBS1 expression is upregulated in the hippocampus of individuals

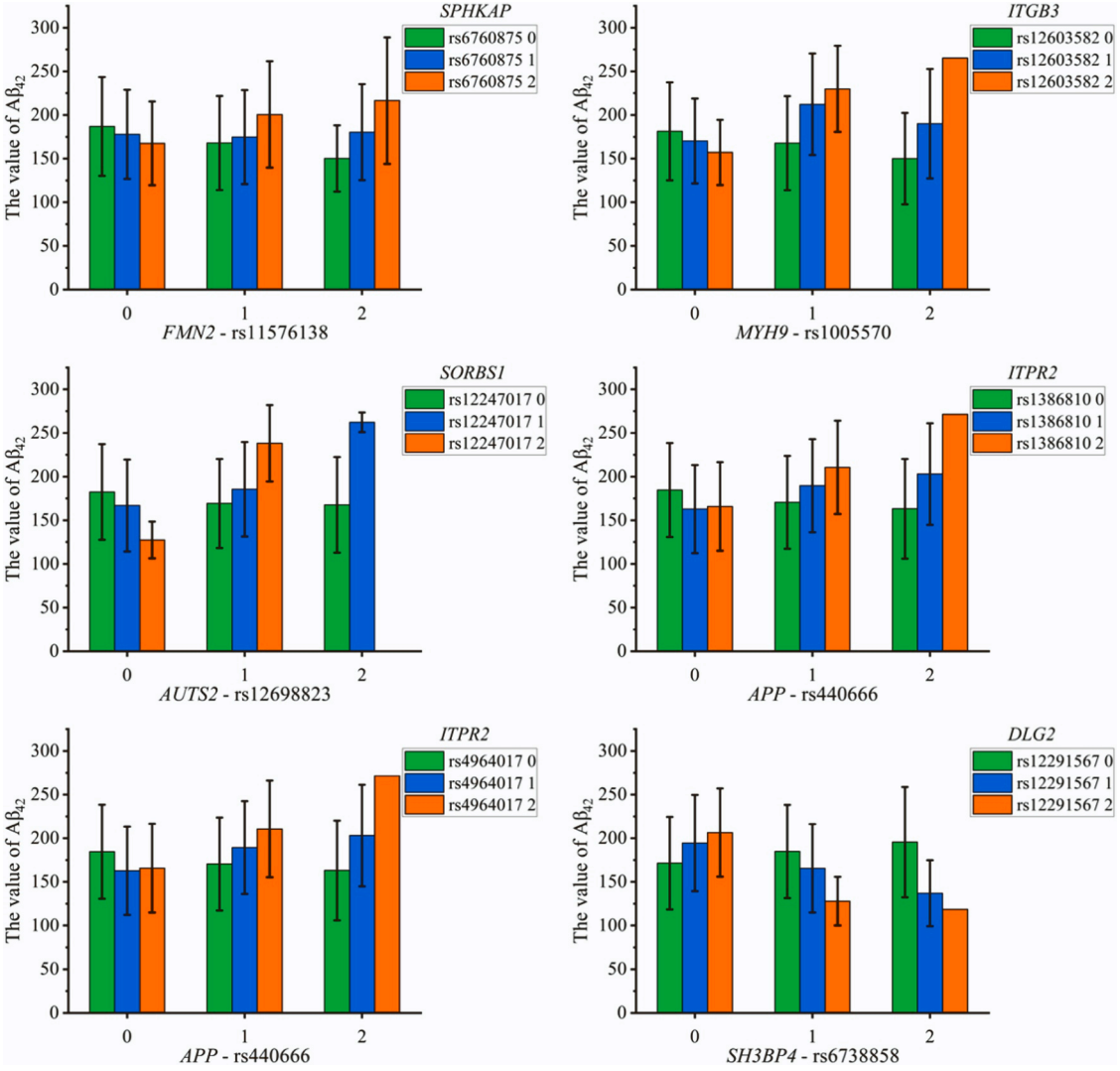

Fig. 6. Pairwise genotype combination chart of the $A\beta_{42}$ value based on 6 pairs of significant genome-wide SNP-SNP interaction effects. The standard deviation is shown as error bars. The *y*-axis represents the value of $A\beta_{42}$ and the *x*-axis represents the pairwise genotype combinations of SNP_1-SNP_2 interactions. Three colors of "green," "blue," and "orange" represent 3 genotypes (AA, Aa, aa) of each single-nucleotide polymorphism, which are numerically represented as (0,1,2), respectively. Abbreviations: APP, amyloid precursor protein; AUTS2, autism susceptibility candidate 2; DLG2, disks large homolog 2; FMN2, formin-2; ITGB3, integrin alpha-V/beta-3; ITPR2, inositol 1,4,5-trisphosphate receptor type; MYH9, myosin heavy chain 9; SH3BP4, SH3 domain-binding protein 4.

suffering from AD (Starnawska et al., 2017), and the effect of down-regulation of *SORBS1* may modify the risk of AD through an Aβ-dependent mechanism (Wang et al., 2006). Autism susceptibility candidate 2 (*AUTS2*) is associated with multiple neurological diseases and is expressed in the central nervous system (Yin et al., 2022). *AUTS2* has been reported as a synapse-regulatory gene for proper synaptic inputs and social communication (Hori et al., 2020). *AUTS2* regulates the actin cytoskeleton to control neuronal migration and neuritogenesis (Hori et al., 2014; Hori and Hoshino, 2017). Synapses are key sites of early pathogenesis in AD, and soluble oligomers of Aβ play a critical role in early AD process. Furthermore, most excitatory synapses in the brain rely on dendritic spines as sites for excitatory neurotransmission, and cellular pathways acting on the actin cytoskeleton dynamically regulate the structure and function of dendritic spines (Penzes and VanLeeuwen, 2011). Therefore, *SORBS1-AUTS2* interaction might be related to regulating actin cytoskeleton and inactivating neuron migration, leading to neuronal aging and cognitive decline in AD.

In summary, 4 pairs of gene-gene interactions might be related to synapse and synaptic activity: *APP-ITPR2*, *MYH9-ITGB3*, *DLG2-SH3BP4*, and *FMN2-SPHKAP*. *SORBS1-AUTS2* interaction might be related to regulating actin cytoskeleton and inactivating neuron migration, which is indirectly associated with the amyloid cascade hypothesis of AD. Since synaptic damage and loss are fundamental to the pathology of AD and an early event in the AD process owing to soluble Aβ, these results are consistent with the analysis of epistatic effects in our study and further support the notion that CSF $A\beta_{42}$ contributes to the detection of potential risk variation associated with it. Moreover, this study also performed PPI network analysis on other 12 pairs of nonoverlapping gene-gene interaction in the PPI subnetwork. The current findings suggest that most of these 12 gene-gene interaction pairs might be related to promoting the catabolism of Aβ (as reported for *APP-DLG2* interaction) (Yu et al., 2017), mediating axon elongation (as reported for *APP-MYH9* interaction) (Javier-Torrent et al., 2019), upregulating reactive microglia in AD (as reported for *APP-ITGB3* interaction) (Neher et al., 2012), remodeling the architecture of actin cytoskeleton (as reported for *FMN2-MYH9* interaction) (Kim et al., 2016), and extracellular vesicles (as reported for *FMN2-SORBS1* interaction) (Muraoka et al., 2021). To our knowledge, these interactions are indirectly associated with synaptic activity, leading to Aβ-mediated cognitive dysfunction, which in turn supports the results of this study. Therefore, the identified subnetwork might

induce synapse loss, damage, dysfunction, and synaptic activity or regulate the actin cytoskeleton, mediate axon elongation, and upregulate microglia in AD, which warrants further investigation.

5. Conclusion

In this study, a linear regression framework was used to perform SNP-SNP interaction detection across the whole genome. Also, we used an efficiently parallel computing approaches based on multi-GPU to solve the issue of the computation burden of searching for all SNP-SNP interaction pairs. Because of the higher sensitivity of CSF $A\beta_{42}$, more statistically significant results were found which allow for a more comprehensive understanding and detecting of potential risk variants both associated with $A\beta_{42}$. To control for any factors outside of genetics that may influence AD and identify potential genetic epistasis that implicated in AD, age, gender, and diagnosis were included in the linear regression models as covariate terms. As expected, the identified 368 statistically significant SNP-SNP interaction pairs explained a relatively high-level variance of $A\beta_{42}$, while their main effects are marginal. In particular, a total of 100 previously reported AD related were replicated, and 5 gene-gene interaction pairs were found to be overlapped with the PPI network. The replicated gene-gene pairs can provide useful clues to the aspect of inducing synaptic loss and dysfunction or other synaptic activity. Our results might have predictive potential on leading to memory decline and cognitive impairment in AD-affected brains. Moreover, the analyses of the identified subnetwork provided further evidence that epistasis interactions between 10 genes (*APP*, *MYH9*, *ITGB3*, *AUTS2*, *SORBS1*, *ITPR2*, *FMN2*, *SPHKAP*, *SH3BP4*, and *DLG2*) that we obtained were important for partially explaining the "missing heritability" of AD. While we have provided exhaust detection of approximately 159 million SNP-SNP pairs in our study, further advances in both computing power and algorithm efficiency will allow for the cross validation in other large and independent datasets in the future.

Funding

This project was supported by the National Natural Science Foundation of China (grant number: 62206044).

Submission declaration and verification

This manuscript has not been published or presented elsewhere in part or in entirety and is not under consideration by another journal. All authors contributed to the manuscript and approved the submitted version. We have read and understood your journal's policies, and we believe that neither the manuscript nor the study violates any of these. There are no conflicts of interest to declare.

Disclosure statement.

The authors have no actual or potential conflicts of interest.

Acknowledgements

The authors acknowledge the Alzheimer's Disease Neuroimaging Initiative database (http://adni.loni.usc.edu/) and Editage (www.editage.com) for English language editing.

CRediT authorship contribution statement

Jin Li: Methodology, Formal analysis, Writing – original draft. **Dandan Chen**: Methodology, Formal analysis, Data curation, Writing – original draft, Visualization. **Qiushi Zhang**: Validation, Writing – review & editing, Project administration. **Hong Liang**: Writing – review & editing, Project administration. **Hongwei Liu**: Data curation, Writing – review & editing. **Yang Xi:** Writing – review & editing, Funding acquisition. **Junfeng Liu**: Writing – review & editing. **Haoran Luo**: Writing – review & editing. **Yiming Wei**: Writing – review & editing.

Author contributions

Jin Li performed the data analysis, and authored the first draft of the manuscript. Dandan Chen designed and conceptualized the study, performed the analyses, authored the first draft of the manuscript, and authored the final manuscript. Qiushi Zhang designed the study and critically revised the manuscript for important intellectual content. Hong Liang performed data analysis and revised the manuscript. Hongwei Liu performed data imputation and contributed preparing figures. Yang Xi and Junfeng Liu assisted in the design of the study. Haoran Luo and Yiming Wei performed literature search and prepared the manuscript.

Supplementary material

Supplementary material associated with this article can be found in the online version at doi:10.1016/j.neurobiolaging.2023.10.003.

References

Abd El Hamid, M.M., Omar, Y.M.K., Shaheen, M., Mabrouk, M.S., 2022. Discovering epistasis interactions in Alzheimer's disease using deep learning model. Gene Rep. 29, 101673 https://doi.org/10.1016/j.genrep.2022.101673.

Abd El Hamid, M.M., Shaheen, M., Omar, Y.M.K., Mabrouk, M.S., 2023. Discovering epistasis interactions in Alzheimer's disease using integrated framework of ensemble learning and multifactor dimensionality reduction (MDR). Ain Shams Eng. J. 14 (7), 101986 https://doi.org/10.1016/j.asej.2022.101986.

Abdullah, M.N., Wah, Y.B., Abdul Majeed, A.B., Zakaria, Y., Shaadan, N., 2022. Identification of blood-based transcriptomics biomarkers for Alzheimer's disease using statistical and machine learning classifier. Inform. Med. Unlocked 33, 101083. https://doi.org/10.1016/j.imu.2022.101083.

Agís-Balboa, R.C., Pinheiro, P.S., Rebola, N., Kerimoglu, C., Benito, E., Gertig, M., Bahari-Javan, S., Jain, G., Burkhardt, S., Delalle, I., Jatzko, A., 2017. Formin 2 links neuropsychiatric phenotypes at young age to an increased risk for dementia. EMBO J. 36 (19), 2815–2828. https://doi.org/10.15252/embj.201796821.

Al-Shammari, R.T., Al-Serri, A.E., Barhoush, S.A., Al-Bustan, S.A., 2022. Identification and characterization of variants in intron 6 of the *LPL* gene locus among a sample of the Kuwaiti population. Genes 13 (4), 664. https://doi.org/10.3390/genes13040664.

Armstrong, R.A., 2009. The molecular biology of senile plaques and neurofibrillary tangles in Alzheimer's disease. Folia Neuropathol. 47 (4), 289–299.

Ashe, P.C., Berry, M.D., Boulton, A.A., 2001. Schizophrenia, a neurodegenerative disorder with neurodevelopmental antecedents. Prog. Neuropsychopharmacol. Biol. Psychiatry 25 (4), 691–707. https://doi.org/10.1016/S0278-5846(01)00159-2.

Bharadwaj, P.R., Dubey, A.K., Masters, C.L., Martins, R.N., Macreadie, I.G., 2009. Aβ aggregation and possible implications in Alzheimer's disease pathogenesis. J. Cell. Mol. Med. 13 (3), 412–421. https://doi.org/10.1111/j.1582-4934.2009.00609.x.

Bondi, M.W., Jak, A.J., Delano-Wood, L., Jacobson, M.W., Delis, D.C., Salmon, D.P., 2008. Neuropsychological contributions to the early identification of Alzheimer's disease. Neuropsychol. Rev. 18 (1), 73–90. https://doi.org/10.1007/s11065-008-9054-1.

Bosch, M., Hayashi, Y., 2012. Structural plasticity of dendritic spines. Curr. Opin. Neurobiol. 22 (3), 383–388. https://doi.org/10.1016/j.conb.2011.09.002.

Cavalcante, G.C., Brito, L.M., Schaan, A.P., Ribeiro-dos-Santos, Â., de Araújo, G.S., on behalf of Alzheimer's Disease Neuroimaging Initiative, 2022. Mitochondrial genetics reinforces multiple layers of interaction in Alzheimer's disease. Biomedicines 10 (4), 880. https://doi.org/10.3390/biomedicines10040880.

Chen, Y., Xu, F., Pian, C., Xu, M., Kong, L., Fang, J., Li, Z., Zhang, L., 2021. EpiMOGA: an epistasis detection method based on a multi-objective genetic algorithm. Genes 12 (2), 191. https://doi.org/10.3390/genes12020191.

Congdon, E.E., Sigurdsson, E.M., 2018. Tau-targeting therapies for Alzheimer disease. Nat. Rev. Neurol. 14 (7), 399–415. https://doi.org/10.1038/s41582-018-0013-z.

Dorostkar, M.M., Zou, C., Blazquez-Llorca, L., Herms, J., 2015. Analyzing dendritic spine pathology in Alzheimer's disease: problems and opportunities. Acta Neuropathol. 130 (1), 1–19. https://doi.org/10.1007/s00401-015-1449-5.

Elman, J.A., Panizzon, M.S., Gustavson, D.E., Franz, C.E., Sanderson-Cimino, M.E., Lyons, M.J., Kremen, W.S., 2020. Amyloid-β positivity predicts cognitive decline but cognition predicts progression to amyloid-β positivity. Biol. Psychiatry 87 (9), 819–828. https://doi.org/10.1016/j.biopsych.2019.12.021.

Hassan, Q., Kerman, K., 2019. Electrochemical approaches for the detection of amyloid-β, tau, and α-synuclein. Curr. Opin. Electrochem. 14, 89–95. https://doi.org/10.1016/j.coelec.2018.12.009.

He, B., Wang, L., Xu, B., Zhang, Y., 2021. Association between CSF Aβ42 and amyloid negativity in patients with different stage mild cognitive impairment. Neurosci. Lett. 754, 135765 https://doi.org/10.1016/j.neulet.2021.135765.

Hibar, D.P., Stein, J.L., Jahanshad, N., Kohannim, O., Hua, X., Toga, A.W., McMahon, K. L., de Zubicaray, G.I., Martin, N.G., Wright, M.J., Weiner, M.W., 2015. Genome-wide interaction analysis reveals replicated epistatic effects on brain structure. Neurobiol. Aging 36, S151–S158. https://doi.org/10.1016/j.neurobiolaging.2014.02.033.
Hohman, T.J., Koran, M.E., Thornton-Wells, T., Alzheimer's Neuroimaging Initiative, 2013. Epistatic genetic effects among Alzheimer's candidate genes. PLoS One 8 (11), e80839. https://doi.org/10.1371/journal.pone.0080839.
Hondius, D.C., Koopmans, F., Leistner, C., Pita-Illobre, D., Peferoen-Baert, R.M., Marbus, F., Paliukhovich, I., Li, K.W., Rozemuller, A.J., Hoozemans, J.J., Smit, A.B., 2021. The proteome of granulovacuolar degeneration and neurofibrillary tangles in Alzheimer's disease. In: Acta Neuropathol., pp. 341–358. https://doi.org/10.1007/s00401-020-02261-4.
Hori, K., Hoshino, M., 2017. Neuronal migration and AUTS2 syndrome. Brain Sci. 7 (5), 54. https://doi.org/10.3390/brainsci7050054.
Hori, K., Nagai, T., Shan, W., Sakamoto, A., Taya, S., Hashimoto, R., Hayashi, T., Abe, M., Yamazaki, M., Nakao, K., Nishioka, T., 2014. Cytoskeletal regulation by AUTS2 in neuronal migration and neuritogenesis. Cell Rep. 9 (6), 2166–2179. https://doi.org/10.1016/j.celrep.2014.11.045.
Hori, K., Yamashiro, K., Nagai, T., Shan, W., Egusa, S.F., Shimaoka, K., Kuniishi, H., Sekiguchi, M., Go, Y., Tatsumoto, S., Yamada, M., 2020. AUTS2 regulation of synapses for proper synaptic inputs and social communication. iScience 23 (6), 101183. https://doi.org/10.1016/j.isci.2020.101183.
Hu, Y., Zhang, H., Liu, B., Gao, S., Wang, T., Han, Z., , International Genomics of Alzheimer's Project (IGAP), Ji, X., Liu, G., 2020. Rs34331204 regulates *TSPAN13* expression and contributes to Alzheimer's disease with sex differences. e95–e95 Brain 143 (11). https://doi.org/10.1093/brain/awaa302.
Islam, M.B., Chowdhury, U.N., Nashiry, M.A., Moni, M.A., 2022. Severity of COVID-19 patients with coexistence of asthma and vitamin D deficiency. Inform. Med. Unlocked 34, 101116. https://doi.org/10.1016/j.imu.2022.101116.
Jansen, I.E., Savage, J.E., Watanabe, K., Bryois, J., Williams, D.M., Steinberg, S., Sealock, J., Karlsson, I.K., Hägg, S., Athanasiu, L., Voyle, N., 2019. Genome-wide meta-analysis identifies new loci and functional pathways influencing Alzheimer's disease risk. Nat. Genet. 51 (3), 404–413. https://doi.org/10.1038/s41588-018-0311-9.
Javier-Torrent, M., Marco, S., Rocandio, D., Pons-Vizcarra, M., Janes, P.W., Lackmann, M., Egea, J., Saura, C.A., 2019. Presenilin/γ-secretase-dependent EphA3 processing mediates axon elongation through non-muscle myosin IIA. eLife 8, e43646. https://doi.org/10.7554/eLife.43646.
John, A., Reddy, P.H., 2021. Synaptic basis of Alzheimer's disease: focus on synaptic amyloid beta, P-tau and mitochondria. Ageing Res. Rev. 65, 101208 https://doi.org/10.1016/j.arr.2020.101208.
Kametani, F., Hasegawa, M., 2018. Reconsideration of amyloid hypothesis and tau hypothesis in Alzheimer's disease. Front. Neurosci. 12, 25 https://doi.org/10.3389/fnins.2018.00025.
Kim, M.H., Kim, J., Hong, H., Lee, S.-H., Lee, J.-K., Jung, E., Kim, J., 2016. Actin remodeling confers BRAF inhibitor resistance to melanoma cells through YAP/TAZ activation. EMBO J. 35 (5), 462–478. https://doi.org/10.15252/embj.201592081.
Kuleshov, M.V., Jones, M.R., Rouillard, A.D., Fernandez, N.F., Duan, Q., Wang, Z., Koplev, S., Jenkins, S.L., Jagodnik, K.M., Lachmann, A., McDermott, M.G., 2016. Enrichr: a comprehensive gene set enrichment analysis web server 2016 update. Nucleic Acids Res. 44 (W1), W90–W97. https://doi.org/10.1093/nar/gkw377.
Law, L.L., Rol, R.N., Schultz, S.A., Dougherty, R.J., Edwards, D.F., Koscik, R.L., Gallagher, C.L., Carlsson, C.M., Bendlin, B.B., Zetterberg, H., Blennow, K., 2018. Moderate intensity physical activity associates with CSF biomarkers in a cohort at risk for Alzheimer's disease. Alzheimers Dement.: Diagn. Assess. Dis. Monit. 10 (1), 188–195. https://doi.org/10.1016/j.dadm.2018.01.001.
Li, J., Zhang, Q., Chen, F., Meng, X., Liu, W., Chen, D., Yan, J., Kim, S., Wang, L., Feng, W., Saykin, A.J., 2017. Genome-wide association and interaction studies of CSF T-tau/Aβ42 ratio in ADNI cohort. Neurobiol. Aging 57, 247.e1–247.e8. https://doi.org/10.1016/j.neurobiolaging.2017.05.007.
Li, J., Zhang, Q., Chen, F., Yan, J., Kim, S., Wang, L., Feng, W., Saykin, A.J., Liang, H., Shen, L., 2015. Genetic interactions explain variance in cingulate amyloid burden: an AV-45 PET genome-wide association and interaction study in the ADNI cohort. BioMed Res. Int. 2015, e647389 https://doi.org/10.1155/2015/647389.
Li, S., Jin, M., Liu, L., Dang, Y., Ostaszewski, B.L., Selkoe, D.J., 2018. Decoding the synaptic dysfunction of bioactive human AD brain soluble Aβ to inspire novel therapeutic avenues for Alzheimer's disease. Acta Neuropathol. Commun. 6 (1), 121 https://doi.org/10.1186/s40478-018-0626-x.
Li, S., Selkoe, D.J., 2020. A mechanistic hypothesis for the impairment of synaptic plasticity by soluble Aβ oligomers from Alzheimer's brain. J. Neurochem. 154 (6), 583–597. https://doi.org/10.1111/jnc.15007.
Lu, J., Fu, J., Zhong, Y., Yang, Q., Huang, J., Li, J., Huo, Y., Zhao, Y., Wan, L., Guo, C., 2018. Association between ABCA1 gene polymorphisms and the therapeutic response to donepezil therapy in Han Chinese patients with Alzheimer's disease. Brain Res. Bull. 140, 1–4. https://doi.org/10.1016/j.brainresbull.2018.03.014.
Mackay, T.F.C., 2014. Epistasis and quantitative traits: using model organisms to study gene–gene interactions. Nat. Rev. Genet. 15 (1), 22–33. https://doi.org/10.1038/nrg3627.
Marchegiani, F., Matacchione, G., Ramini, D., Marcheselli, F., Recchioni, R., Casoli, T., Mercuri, E., Lazzarini, M., Giorgetti, B., Cameriere, V., Paolini, S., 2019. Diagnostic performance of new and classic CSF biomarkers in age-related dementias. Aging (Albany NY) 11 (8), 2420–2429. https://doi.org/10.18632/aging.101925.
Mencer, S., Kartawy, M., Lendenfeld, F., Soluh, H., Tripathi, M.K., Khaliulin, I., Amal, H., 2021. Proteomics of autism and Alzheimer's mouse models reveal common alterations in mTOR signaling pathway. Transl. Psychiatry 11 (1), 480. https://doi.org/10.1038/s41398-021-01578-2.
Meyers, E.A., Amouyel, P., Bovenkamp, D.E., Carrillo, M.C., De Buchy, G.D., Dumont, M., Fillit, H., Friedman, L., Henderson-Begg, G., Hort, J., Murtishaw, A., 2022. Commentary: global Alzheimer's disease and Alzheimer's disease related dementia research funding organizations support and engage the research community throughout the COVID-19 pandemic. Alzheimers Dement. 18 (5), 1067–1070. https://doi.org/10.1002/alz.12472.
Miron, J., Picard, C., Nilsson, N., Frappier, J., Dea, D., Théroux, L., , Alzheimer's Disease Neuroimaging Initiative, United Kingdom Brain Expression Consortium, Poirier, J., 2018. *CDK5RAP2* gene and tau pathophysiology in late-onset sporadic Alzheimer's disease. Alzheimers Dement. 14 (6), 787–796. https://doi.org/10.1016/j.jalz.2017.12.004.
Moore, J.H., 2005. A global view of epistasis. Nat. Genet. 37 (1), 13–14. https://doi.org/10.1038/ng0105-13.
Muraoka, S., Jedrychowski, M.P., Iwahara, N., Abdullah, M., Onos, K.D., Keezer, K.J., Hu, J., Ikezu, S., Howell, G.R., Gygi, S.P., Ikezu, T., 2021. Enrichment of neurodegenerative microglia signature in brain-derived extracellular vesicles isolated from Alzheimer's disease mouse models. J. Proteome Res. 20 (3), 1733–1743. https://doi.org/10.1021/acs.jproteome.0c00934.
Neher, J.J., Neniskyte, U., Brown, G.C., 2012. Primary phagocytosis of neurons by inflamed microglia: potential roles in neurodegeneration. Front. Pharmacol. 3, 27. https://doi.org/10.3389/fphar.2012.00027.
Nguyen, H.L., Thi Minh Thu, T., Minh Truong, P., Lan, P.D., Man, V.H., Nguyen, P.H., Tu, L.A., Chen, Y.-C., Li, M.S., 2016. Aβ41 aggregates more like Aβ40 than like Aβ42: in silico and in vitro study. J. Phys. Chem. B 120 (30), 7371–7379. https://doi.org/10.1021/acs.jpcb.6b06368.
Ownby, R.L., Crocco, E., Acevedo, A., John, V., Loewenstein, D., 2006. Depression and risk for Alzheimer disease: systematic review, meta-analysis, and metaregression analysis. Arch. Gen. Psychiatry 63 (5), 530–538. https://doi.org/10.1001/archpsyc.63.5.530.
Penzes, P., VanLeeuwen, J.-E., 2011. Impaired regulation of synaptic actin cytoskeleton in Alzheimer's disease. Brain Res. Rev. 67 (1–2), 184–192. https://doi.org/10.1016/j.brainresrev.2011.01.003.
Pfeil, J., Hoenig, M.C., Doering, E., van Eimeren, T., Drzezga, A., Bischof, G.N., 2021. Unique regional patterns of amyloid burden predict progression to prodromal and clinical stages of Alzheimer's disease. Neurobiol. Aging 106, 119–129. https://doi.org/10.1016/j.neurobiolaging.2021.06.014.
Piccioni, G., Mango, D., Saidi, A., Corbo, M., Nisticò, R., 2021. Targeting microglia-synapse interactions in Alzheimer's disease. Int. J. Mol. Sci. 22 (5), 2342. https://doi.org/10.3390/ijms22052342.
Piñero, J., Ramírez-Anguita, J.M., Saüch-Pitarch, J., Ronzano, F., Centeno, E., Sanz, F., Furlong, L.I., 2019. The DisGeNET knowledge platform for disease genomics: 2019 update. Nucleic Acids Res. 48, 845–855. https://doi.org/10.1093/nar/gkz1021.
Prokopenko, D., Lee, S., Hecker, J., Mullin, K., Morgan, S., Katsumata, Y., Alzheimer's Disease Neuroimaging Initiative (ADNI), 2022. Region-based analysis of rare genomic variants in whole-genome sequencing datasets reveal two novel Alzheimer's disease-associated genes: DTNB and DLG2. Mol. Psychiatry 27 (4), 1963–1969. https://doi.org/10.1038/s41380-022-01475-0.
Puglielli, L., Tanzi, R.E., Kovacs, D.M., 2003. Alzheimer's disease: the cholesterol connection. Nat. Neurosci. 6 (4), 345–351. https://doi.org/10.1038/nn0403-345.
Quon, D., Wang, Y., Catalano, R., Scardina, J.M., Murakami, K., Cordell, B., 1991. Formation of β-amyloid protein deposits in brains of transgenic mice. Nature 352 (6332), 239–241. https://doi.org/10.1038/352239a0.
Rajmohan, R., Reddy, P.H., 2017. Amyloid-beta and phosphorylated tau accumulations cause abnormalities at synapses of Alzheimer's disease neurons. J. Alzheimers Dis. 57 (4), 975–999. https://doi.org/10.3233/JAD-160612.
Ridge, P.G., Mukherjee, S., Crane, P.K., Kauwe, J.S., Alzheimer's Disease Genetics Consortium, 2013. Alzheimer's disease: analyzing the missing heritability. PloS One 8 (11), e79771. https://doi.org/10.1371/journal.pone.0079771.
Ropacki, S.A., Jeste, D.V., 2005. Epidemiology of and risk factors for psychosis of Alzheimer's disease: a review of 55 studies published from 1990 to 2003. Am. J. Psychiatry 162 (11), 2022–2030. https://doi.org/10.1176/appi.ajp.162.11.2022.
Russ, D., Williams, J.A., Cardoso, V.R., Bravo-Merodio, L., Pendleton, S.C., Aziz, F., Acharjee, A., Gkoutos, G.V., 2022. Evaluating the detection ability of a range of epistasis detection methods on simulated data for pure and impure epistatic models. PLoS One 17 (2), e0263390. https://doi.org/10.1371/journal.pone.0263390.
Safari-Alighiarloo, N., Taghizadeh, M., Rezaei-Tavirani, M., Goliaei, B., Peyvandi, A.A., 2014. Protein-protein interaction networks (PPI) and complex diseases. Gastroenterol. Hepatol. Bed Bench 7 (1), 17–31.
Sethi, M.K., Zaia, J., 2017. Extracellular matrix proteomics in schizophrenia and Alzheimer's disease. Anal. Bioanal. Chem. 409 (2), 379–394. https://doi.org/10.1007/s00216-016-9900-6.
Shobab, L.A., Hsiung, G.-Y.R., Feldman, H.H., 2005. Cholesterol in Alzheimer's disease. Lancet Neurol. 4 (12), 841–852. https://doi.org/10.1016/S1474-4422(05)70248-9.
Sims, R., Hill, M., Williams, J., 2020. The multiplex model of the genetics of Alzheimer's disease. Nat. Neurosci. 23 (3), 311–322. https://doi.org/10.1038/s41593-020-0599-5.
Smith, A.S., Pal, K., Nowak, R.B., Demenko, A., Zaninetti, C., Da Costa, L., Favier, R., Pecci, A., Fowler, V.M., 2019. *MYH9*-related disease mutations cause abnormal red blood cell morphology through increased myosin-actin binding at the membrane. Am. J. Hematol. 94 (6), 667–677. https://doi.org/10.1002/ajh.25472.
Starnawska, A., Tan, Q., McGue, M., Mors, O., Børglum, A.D., Christensen, K., Nyegaard, M., Christiansen, L., 2017. Epigenome-wide association study of cognitive functioning in middle-aged monozygotic twins. Front. Aging Neurosci. 9, 413 https://doi.org/10.3389/fnagi.2017.00413.
The Synaptic Health Endpoints Working Group, Colom-Cadena, M., Spires-Jones, T., Zetterberg, H., Blennow, K., Caggiano, A., DeKosky, S.T., Fillit, H., Harrison, J.E.,

Schneider, L.S., Scheltens, P., de Haan, W., 2020. The clinical promise of biomarkers of synapse damage or loss in Alzheimer's disease. Alzheimers Res. Ther. 12 (1), 21 https://doi.org/10.1186/s13195-020-00588-4.

The Texas Alzheimer Research and Care Consortium, Szigeti, K., Lal, D., Li, Y., Doody, R. S., Wilhelmsen, K., Yan, L., Liu, S., Ma, C., 2012. Genome-wide scan for copy number variation association with age at onset of Alzheimer's disease. J. Alzheimers Dis. 33 (2), 517–523. https://doi.org/10.3233/JAD-2012-121285.

Tian, M.-L., Ni, X.-N., Li, J.-Q., Tan, C.-C., Cao, X.-P., Tan, L., for the Alzheimer's Disease Neuroimaging Initiative, 2019. A candidate regulatory variant at the TREM gene cluster confer Alzheimer's disease risk by modulating both amyloid-β pathology and neuronal degeneration. Front. Neurosci. 13, 742 https://doi.org/10.3389/fnins.2019.00742.

Vance, E., Gonzalez Murcia, J.D., Miller, J.B., Staley, L., Crane, P.K., Mukherjee, S., Kauwe, J.S.K., 2020. Failure to detect synergy between variants in transferrin and hemochromatosis and Alzheimer's disease in large cohort. Neurobiol. Aging 89, 142.e9–142.e12. https://doi.org/10.1016/j.neurobiolaging.2020.01.013.

Wang, H., Bennett, D.A., De Jager, P.L., Zhang, Q.-Y., Zhang, H.-Y., 2021. Genome-wide epistasis analysis for Alzheimer's disease and implications for genetic risk prediction. Alzheimers Res. Ther. 13 (1), 55 https://doi.org/10.1186/s13195-021-00794-8.

Wang, J., Grupe, A., Li, Y., Nowotny, P., Goate, A., 2006. P1–299: sorbs 1, a candidate gene for the chromosome 10 late onset Alzheimer's disease locus. Alzheimers Dement. 2 (3S_Part_6), 184. https://doi.org/10.1016/j.jalz.2006.05.676.

Wang, Q., Zhang, Q., Meng, F., Li, B., 2023. Objective-Hierarchy Based Large-Scale Evolutionary Algorithm for Improving Joint Sparsity-Compression of Neural Network. Inf. Sci. 640, 119095.

Xie, Z., Bailey, A., Kuleshov, M.V., Clarke, D.J.B., Evangelista, J.E., Jenkins, S.L., Lachmann, A., Wojciechowicz, M.L., Kropiwnicki, E., Jagodnik, K.M., Jeon, M., 2021. Gene Set Knowledge Discovery with Enrichr. Curr. Protoc. 1 (3), e90. https://doi.org/10.1002/cpz1.90.

Yang, J., Hongbin Yang, Y.L., Xia Li, L.Q., Huifang Lou, S.D., Wang, Hao, 2016. Astrocytes contribute to synapse elimination via type 2 inositol 1,4,5-trisphosphate receptor-dependent release of ATP. eLife 5, e15043. https://doi.org/10.7554/eLife.15043.

Yin, Z., Guo, X., Qi, Y., Li, P., Liang, S., Xu, X., Shang, X., 2022. Dietary restriction and rapamycin affect brain aging in mice by attenuating age-related DNA methylation changes. Genes 13 (4), 699. https://doi.org/10.3390/genes13040699.

Yu, L., Liu, Y., Yang, H., Zhu, X., Cao, X., Gao, J., Zhao, H., Xu, Y., 2017. PSD-93 attenuates amyloid-β-mediated cognitive dysfunction by promoting the catabolism of amyloid-β. J. Alzheimers Dis. 59 (3), 913–927. https://doi.org/10.3233/JAD-170320.

Zajac, D.J., Simpson, J., Zhang, E., Parikh, I., Estus, S., 2023. Expression of INPP5D isoforms in human brain: impact of Alzheimer's disease neuropathology and genetics. Genes 14 (3), 763. https://doi.org/10.3390/genes14030763.

Zhang, Q., Liu, H., Ao, L., Liang, H., Chen, D., 2022. A GPU-based approach for detectinggenome-wide SNP-SNP interactions of quantitative trait in ADNI cohorts. IEEE International Conference on Bioinformatics and Biomedicine (BIBM). IEEE, LasVegas, NV, USA, pp. 2564–2570. https://doi.org/10.1109/BIBM55620.2022.9995349.

Zhang, Y., McLaughlin, R., Goodyer, C., LeBlanc, A., 2002. Selective cytotoxicity of intracellular amyloid β peptide1–42 through P53 and bax in cultured primary human neurons. J. Cell Biol. 156 (3), 519–529.